Journal of Earth Science, *Vol. 30*, *No. 4*, *p. 834–842*, *August 2019* *ISSN 1674-487X*
Printed in China
https://doi.org/10.1007/s12583-017-0939-x

Effect of Beam Current and Diameter on Electron Probe Microanalysis of Carbonate Minerals

Xing Zhang[1], **Shuiyuan Yang***[1], **He Zhao**[2], **Shaoyong Jiang**[1, 3, 4], **Ruoxi Zhang**[1], **Jing Xie**[5]

1. *State Key Laboratory of Geological Processes and Mineral Resources*, *China University of Geosciences*, *Wuhan* 430074, *China*
2. *College of Earth Sciences*, *Chengdu University of Technology*, *Chengdu* 610059, *China*
3. *Faculty of Earth Resources and Collaborative Innovation Center for Scarce and Strategic Mineral Resources*, *China University of Geosciences*, *Wuhan* 430074, *China*
4. *State Key Laboratory for Mineral Deposits Research*, *School of Earth Sciences and Engineering*, *Nanjing University*, *Nanjing* 210093, *China*
5. *Institute of Tibetan Plateau Research*, *Chinese Academy of Sciences*, *Beijing* 100085, *China*

Xing Zhang: https://orcid.org/0000-0002-1229-569X; Shuiyuan Yang: https://orcid.org/0000-0003-3594-8865

ABSTRACT: The effect of operating conditions on the time-dependent X-ray intensity variation is of great importance for the optimal EPMA conditions for accurate determinations of various elements in carbonate minerals. Beam diameters of 0, 1, 2, 5, 10, 15, and 20 μm, and beam currents of 3, 5, 10, 20, and 50 nA were tested. Ca, Mg, Zn, and Sr were found to be more sensitive to electron beam irradiation as compared to other elements, and small currents and large beam diameters minimized the time-dependent X-ray intensity variations. We determined the optimal EPMA operating conditions for elements in carbonate: 10 μm and 5 nA for calcite; 10 μm and 10 nA for dolomite; 5 μm and 10 nA or 10 μm and 20 nA for strontianite; and 20 nA and 5 μm for other carbonate. Elements sensitive to electron beam irradiation should be determined first. In addition, silicate minerals are preferred as standards rather than carbonate minerals.

KEY WORDS: carbonate minerals, electron probe microanalysis, characteristic X-ray, time-dependent intensity, beam current, beam diameter.

0 INTRODUCTION

Carbonate minerals (MCO_3), including mainly calcite [$CaCO_3$], dolomite [$CaMg(CO_3)_2$], magnesite [$MgCO_3$], siderite [$FeCO_3$], rhodochrosite [$MnCO_3$], smithsonite [$ZnCO_3$], malachite [$Cu_2CO_3(OH)_2$], azurite [$Cu_3(CO_3)_2(OH)_2$], strontianite [$SrCO_3$], and cerussite [$PbCO_3$], are widely distributed in geological materials. The accurate determination of elemental content of carbonate minerals is important in earth science. Electron probe microanalysis (EPMA) is the most commonly used analytical method for the determination of elements in solid materials (Zhao et al., 2015; McGee and Keil, 2001; Sweatman and Long, 1969) and has been widely utilized in geological research (Ye et al., 2017; Zhang et al., 2017; Zhao et al., 2017; Yang et al., 2015a, b; Yang and Jiang, 2013, 2012). However, many geological materials have proven to be sensitive to electron beam irradiation, leading to changes in the time-dependent intensity (TDI) of elemental X-rays in materials such as glass (Humphreys et al., 2006; Morgan and London, 2005; Jurek and Gedeon, 2003; Morgan and London, 1996; Spray and Rae, 1995), apatite (Stock et al., 2015; Goldoff et al., 2012; Marks et al., 2012; Henderson, 2011; Stormer et al., 1993), carbonate minerals (Lane and Dalton, 1994), feldspar, fluorite, zeolite, and other hydrous minerals.

Element migration in carbonate minerals under electron beam irradiation has been discovered a long time ago (Lane and Dalton, 1994; Essene, 1983). Essene (1983) carried out an EPMA of carbonate minerals to determine whether the samples or standards were damaged by electron beam irradiation. However, the EPMA operating conditions and the standard used significantly affect the test results. A complete and detailed study of the optimal analytical conditions for each carbonate mineral has not yet been reported. In this work, we aimed to investigate the effect of the operating conditions on the time-dependent X-ray intensity changes and optimize the EPMA conditions for elemental determination in carbonate minerals. Moreover, the selection of standards is discussed to finally obtain the optimal EPMA operating conditions for carbonate mineral analysis.

*Corresponding author: shuiyuanyang@cug.edu.cn

Manuscript received March 26, 2017.
Manuscript accepted December 2, 2017.

1 ANALYTICAL METHOD

1.1 Sample Preparation

The samples used in this study are shown in Table 1. Prior to analysis, the samples were coated with a thin conductive carbon film. The precautions suggested by Zhang and Yang (2016) were used to minimize the differences in carbon film thickness

and therefore in X-ray excitation intensity (Kerrick et al., 1973) among the samples, to obtain an almost uniform coating of ca. 20 nm.

1.2 EPMA for TDI Variations of Elemental X-Rays

The characteristic X-ray intensities of elements in carbonate minerals were determined at the State Key Laboratory of Geological Processes and Mineral Resources, China University of Geosciences (Wuhan), using a JEOL JXA-8100 electron probe micro analyzer equipped with four wavelength-dispersive spectrometers. The "chart record" function in the electronic probe software was used to record the TDI variations of elemental X-rays upon irradiation with different beam diameters and under different current conditions. Under all conditions, the total data acquisition time was 360 s in consecutive 3 s counting intervals (no beam blanking). The operating conditions were as follows: an acceleration voltage of 10, 15, 20 kV for Ca and C, an acceleration voltage of 15 kV for Mg, Fe, Mn, Sr and Pb, and 20 kV for Cu and Zn, a beam current of 3, 5, 10, 20, or 50 nA, and a beam diameter of 0, 1, 2, 5, 10, 15, or 20 μm. The X-ray intensities of Ca (Kα, PETJ), Mg (Kα, TAP), Fe (Kα, LIFH), Mn (Kα, LIFH), Cu (Kα, LIFH), Zn (Kα, LIFH), Sr (Lα, TAP), Pb (Mα, PETJ), and C (Kα, LDE2H) were investigated. The detailed test conditions are summarized in Table 1.

Table 1 Clinopyroxene composition (wt.%)

Sample No.	Mineral name	Beam diameter (μm)	Beam current (nA)	Acceleration voltage (kV)	Analytical element	Sample No.	Mineral name	Beam diameter (μm)	Beam current (nA)	Acceleration voltage (kV)	Analytical element
CC-1	Calcite	0	10	15	Ca, C	CC-15	Rhodochrosite	5	5	15	Mn
CC-1	Calcite	1	10	15	Ca, C	CC-15	Rhodochrosite	5	10	15	Mn
CC-1	Calcite	2	10	15	Ca, C	CC-15	Rhodochrosite	5	20	15	Mn
CC-1	Calcite	5	10	15	Ca, C	CC-15	Rhodochrosite	5	50	15	Mn
CC-1	Calcite	5	20	10	Ca, C	CC-15	Rhodochrosite	10	20	15	Mn
CC-1	Calcite	5	20	15	Ca, C	CC-13	Smithsonite	0	20	20	Zn
CC-1	Calcite	5	20	20	Ca, C	CC-13	Smithsonite	1	20	20	Zn
CC-1	Calcite	10	3	15	Ca, C	CC-13	Smithsonite	2	20	20	Zn
CC-1	Calcite	10	5	15	Ca, C	CC-13	Smithsonite	5	5	20	Zn
CC-1	Calcite	10	10	15	Ca, C	CC-13	Smithsonite	5	10	20	Zn
CC-1	Calcite	10	20	15	Ca, C	CC-13	Smithsonite	5	20	20	Zn
CC-1	Calcite	15	10	15	Ca, C	CC-13	Smithsonite	5	50	20	Zn
CC-1	Calcite	20	10	15	Ca, C	CC-13	Smithsonite	10	20	20	Zn
CC-2	Calcite	20	10	15	Ca, C	CC-12	Smithsonite	1	20	20	Zn
CC-3	Calcite	10	20	15	Ca, C	CC-12	Smithsonite	2	20	20	Zn
CC-3	Calcite	20	10	15	Ca, C	CC-11	Malachite	0	20	20	Cu
CC-4	Calcite	20	10	15	Ca, C	CC-11	Malachite	1	20	20	Cu
CC-5	Calcite	20	10	15	Ca, C	CC-11	Malachite	2	20	20	Cu
CC-6	Dolomite	0	10	15	Ca, Mg, C	CC-11	Malachite	5	5	20	Cu
CC-6	Dolomite	1	10	15	Ca, Mg, C	CC-11	Malachite	5	10	20	Cu
CC-6	Dolomite	2	10	15	Ca, Mg, C	CC-11	Malachite	5	20	20	Cu
CC-6	Dolomite	5	10	15	Ca, Mg, C	CC-11	Malachite	5	50	20	Cu
CC-6	Dolomite	10	5	15	Ca, Mg, C	CC-11	Malachite	10	20	20	Cu
CC-6	Dolomite	10	10	15	Ca, Mg, C	CC-9	Azurite	0	20	20	Cu
CC-6	Dolomite	10	15	15	Ca, Mg, C	CC-9	Azurite	1	20	20	Cu
CC-6	Dolomite	10	20	15	Ca, Mg, C	CC-9	Azurite	2	20	20	Cu
CC-6	Dolomite	20	10	15	Ca, Mg, C	CC-9	Azurite	5	5	20	Cu
CC-7	Dolomite	10	20	15	Ca, Mg, C	CC-9	Azurite	5	10	20	Cu
CC-21	Dolomite	10	20	15	Ca, Mg, C	CC-9	Azurite	5	20	20	Cu
CC-19	Magnesite	0	20	15	Mg	CC-9	Azurite	5	50	20	Cu
CC-19	Magnesite	1	20	15	Mg	CC-9	Azurite	10	20	20	Cu
CC-19	Magnesite	2	20	15	Mg	CC-20	Strontianite	0	20	15	Sr
CC-19	Magnesite	5	5	15	Mg	CC-20	Strontianite	1	20	15	Sr
CC-19	Magnesite	5	10	15	Mg	CC-20	Strontianite	2	20	15	Sr
CC-19	Magnesite	5	20	15	Mg	CC-20	Strontianite	5	5	15	Sr
CC-19	Magnesite	5	50	15	Mg	CC-20	Strontianite	5	10	15	Sr
CC-19	Magnesite	10	20	15	Mg	CC-20	Strontianite	5	20	15	Sr
CC-18	Siderite	0	20	15	Fe	CC-20	Strontianite	5	50	15	Sr
CC-18	Siderite	1	20	15	Fe	CC-20	Strontianite	10	20	15	Sr
CC-18	Siderite	2	20	15	Fe	CC-16	Cerussite	0	20	15	Pb
CC-18	Siderite	5	5	15	Fe	CC-16	Cerussite	1	20	15	Pb
CC-18	Siderite	5	10	15	Fe	CC-16	Cerussite	2	20	15	Pb
CC-18	Siderite	5	20	15	Fe	CC-16	Cerussite	5	5	15	Pb
CC-18	Siderite	5	50	15	Fe	CC-16	Cerussite	5	10	15	Pb
CC-18	Siderite	10	20	15	Fe	CC-16	Cerussite	5	20	15	Pb
CC-15	Rhodochrosite	0	20	15	Mn	CC-16	Cerussite	5	50	15	Pb
CC-15	Rhodochrosite	1	20	15	Mn	CC-16	Cerussite	10	20	15	Pb
CC-15	Rhodochrosite	2	20	15	Mn						

2 RESULTS AND DISCUSSION

EPMA is based on the principle that when a solid material is bombarded with an accelerated and focused electron beam, the incident electron beam causes each element in the sample to emit X-rays at a characteristic frequency, which can be detected by the electron probe micro analyzer. After measuring the X-ray counts of an element in both unknowns and standards using the same instrument, the element content in the unknowns can be obtained by the following formula (Sweatman and Long, 1969)

$$C_{\mathrm{A}}^{\mathrm{unk}} = C_{\mathrm{A}}^{\mathrm{std}} \times \frac{I_{\mathrm{A}}^{\mathrm{unk}}}{I_{\mathrm{A}}^{\mathrm{std}}} \times \frac{\mathrm{ZAF}^{\mathrm{unk}}}{\mathrm{ZAF}^{\mathrm{std}}}$$

where C_{A} is mass concentration of element A (wt.%), I_{A} is X-ray intensity of element A (cps/μA), std is standard specimen, unk is unknown specimen, ZAF is correction factor.

The formula shows that characteristic elemental X-ray intensities are key in accurately determining unknown element contents. In the following, we will discuss the effect of beam diameter and current density on the TDI variation of elemental X-rays in carbonate minerals.

2.1 Effect of Accelerating Voltage on the TDI Variation of Elemental X-Rays

In this study, Ca and C in calcite were selected to investigate the effect of accelerating voltage on the time-dependent X-ray intensity variation. The accelerating voltage are 10, 15, and 20 kV, the beam current is 20 nA, the beam diameter is 5 μm, and the results are shown in Fig. 1. When the accelerating voltage are 15 and 20 kV, the Ca X-ray intensity increases during the first 30 s of beam irradiation, and then the intensity decreases in the next 30 s and then remain constant over the following 360 s of beam irradiation (Fig. 1a). With 10 kV acceleration voltage, the Ca X-ray intensity became nearly constant. The C X-ray intensities gradually decline (Fig. 1b). It seems that the lower accelerating voltage can reduce changes in TDI of Ca and C in calcite. However, during the EPMA of carbonate minerals, other cautions such as Fe and Mn usually involve in the analysis. In EPMA, the accelerating voltage is desirable to set higher than 2 or 3 times of excitation energy of the element interested. Consequently, the accelerating voltage of 15 kV is recommended during the EPMA of carbonate minerals (and 20 kV should be used when Cu is involved).

2.2 Effect of Beam Diameter on the TDI Variation of Elemental X-Rays

We investigated the effect of beam diameter on the time-dependent X-ray intensity variation of elements in carbonate minerals, and representative results are shown in Figs. 2 and 3. Analysis of carbonate minerals irradiated with a 15 kV accelerating voltage and a 10 nA beam current with different beam diameters of 0, 1, 2, 5, 10, 15, and 20 μm showed TDI variations in Ca and C X-ray intensities. We found that, in calcite, the characteristic Ca and C X-ray intensities changed significantly using small beam spots (0, 1, and 2 μm) (Figs. 2a, 2b). The intensity of Ca fluctuated slightly using beam diameters of 10, 15, and 20 μm as compared with the use of a 5 μm beam diameter (Fig. 2a). Using a 0, 1, or 2 μm electron beam spot, the Ca X-ray intensity in calcite fluctuated largely and irregularly, first increasing and then decreasing. Conversely, the Ca X-ray intensity increased steadily using 5, 10, 15, and 20 μm diameter spots, with a smaller magnitude of change for spot diameters smaller than 20 μm. Moreover, for all beam diameters, calcite showed fluctuations in C X-ray intensity (Fig. 2b), with the widest variation observed using a 0 μm diameter spot, which generated an irregular fluctuation. Using 1, 2, 5, 10, 15, and 20 μm beam diameters, the C X-ray intensity decreased steadily.

For dolomite, we observed TDI variations in Ca, Mg, and C X-ray intensities using beam diameters of 0, 1, 2, 5, 10, and 20 μm, under an acceleration voltage of 15 kV and a current of 10 nA (Figs. 2c–2e). The Ca and Mg X-ray intensities increased more quickly with the use of a focused beam spot (0 μm) as compared with the use of 1, 2, and 5 μm beam diameters (Figs. 2c, 2d). When analyzed with a 10 or 20 μm electron beam spot, the Ca and Mg X-ray intensities remained constant. The C X-ray intensity was inversely proportional to those of Ca and Mg, and decreased most quickly using a 0 μm beam diameter (Fig. 2e).

For other types of carbonate minerals, a 20 nA beam current and 0, 1, 2, 5, and 10 μm beam diameters were used to test the TDI variations of element M, and the results are shown in Fig. 3. In magnesite, the X-ray intensity of Mg increased steadily using a 0 μm diameter spot. When analyzed with a 1 or 2 μm diameter spot, the Mg intensity remained constant for 120 s and then slightly increased between 120 and 360 s, whereas a constant intensity was observed using beams of 5 and 10 μm diameter (Fig. 3a). The X-ray intensities of Fe in siderite (Fig. 3b), Mn in rhodochrosite (Fig. 3c), and Pb in cerussite (Fig. 3h) remained constant for 360 s using 0, 1, 2, 5, and 10 μm diameter spots. The Zn X-ray intensity in smithsonite (Fig. 3d) showed an increase of about 35%–40% over 360 s when using a beam diameter of 0 or 1 μm. On the other hand, using a 2 or 5 μm beam diameter the intensity was initially constant (about 120–180 s) and then steadily increased, whereas it remained constant with a 10 μm beam diameter (Fig. 3d). The Sr X-ray intensity of strontianite (Fig. 3g) increased steadily and similarly using beam diameters of 0, 1, or 2 μm beam diameter. The Sr intensity slightly increased when a 5 μm beam diameter was used, and remained constant with a 10 μm diameter spot. The TDI variations of Cu in malachite (Fig. 3e) and azurite (Fig. 3f) are similar. The Cu intensity decreases steadily using 0 μm diameter spots. When analyzed with a 1 or 2 μm diameter spot, the Cu intensity decreased slightly in malachite and more significantly in azurite, whereas it remained constant using a 5 or 10 μm beam diameter.

In summary, element M in carbonate minerals showed an increasing X-ray intensity under electron beam irradiation (except for Cu), whereas element C showed an opposite trend. Small beam diameters resulted in variable X-ray intensities, whereas constant X-ray intensities were obtained with large beam diameters. This is consistent with previous research results on glass and apatite (Goldoff et al., 2012; Morgan and London, 2005; Morgan and London, 1996; Stormer et al., 1993).

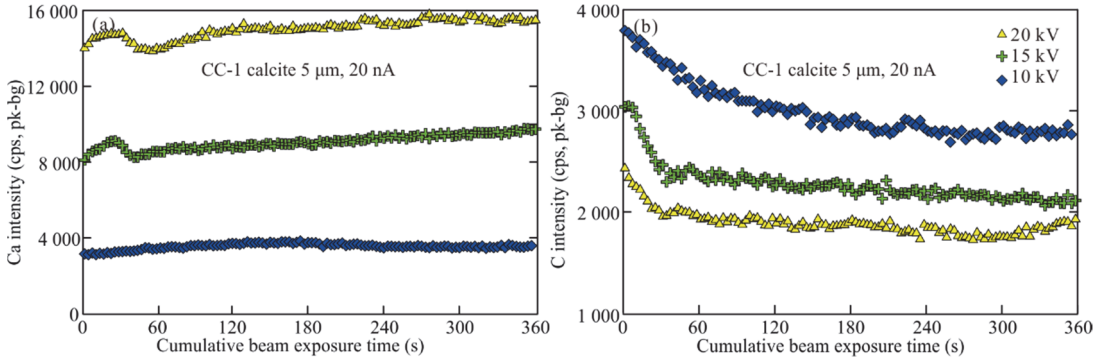

Figure 1. Effect of accelerating voltage on the X-ray TDI variations of Ca (a) and C (b) in calcite.

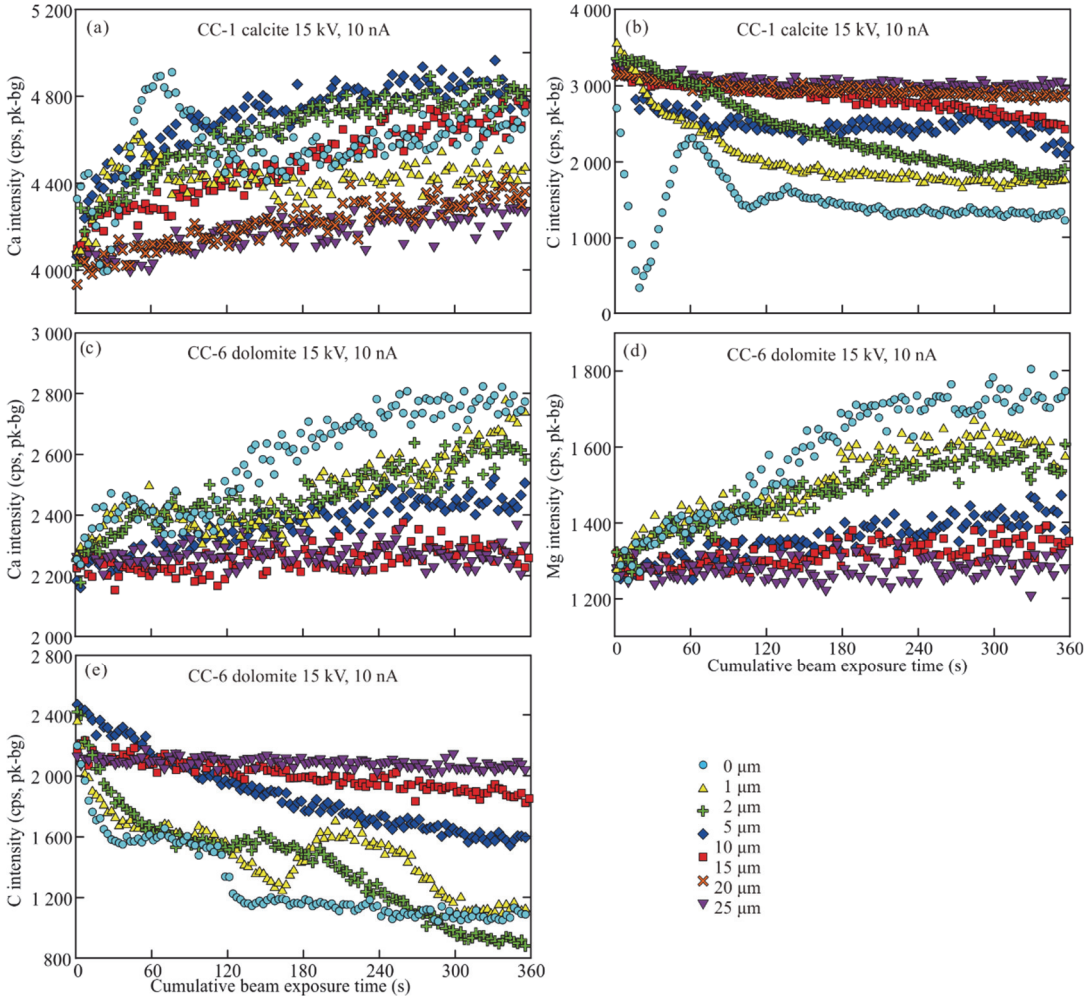

Figure 2. Effect of beam diameter on the X-ray TDI variations of Ca and C in calcite (a)–(b), and Ca, Mg, and C in dolomite (c)–(e).

2.3 Effect of Beam Current on the TDI Variation of Elemental X-Rays

A low beam current is often used to minimize X-ray intensity fluctuations; on the other hand, increasing the beam current will increase the X-ray intensity, thereby improving the precision of analysis but only provided that the TDI remains constant (Goldoff et al., 2012; Stormer et al., 1993). Thus, experiments were carried out to assess the TDI variation of elemental X-rays in carbonate minerals using different beam currents (3, 5, 10, 20, and 50 nA). We used a beam diameter of 10 μm for calcite and dolomite, and of 5 μm for other carbonate minerals.

For calcite (Fig. 4a), we found that, with a 20 nA current, the TDI of Ca X-ray changed dramatically, increasing by about 11% in the first 180 s and then rapidly decreasing to below the initial value. On the other hand, using a 10 nA current, the Ca X-ray intensity increased steadily by about 20% over 360 s, whereas with a beam current of 5 or 3 nA, the Ca intensity remained nearly constant. The TDI variations of C in calcite (Fig. 4a) showed an opposite trend. Using a 20 nA beam current, the characteristic C X-ray intensity decreased over the first 180 s and then slightly increased, whereas it was most stable with a 3 nA beam current.

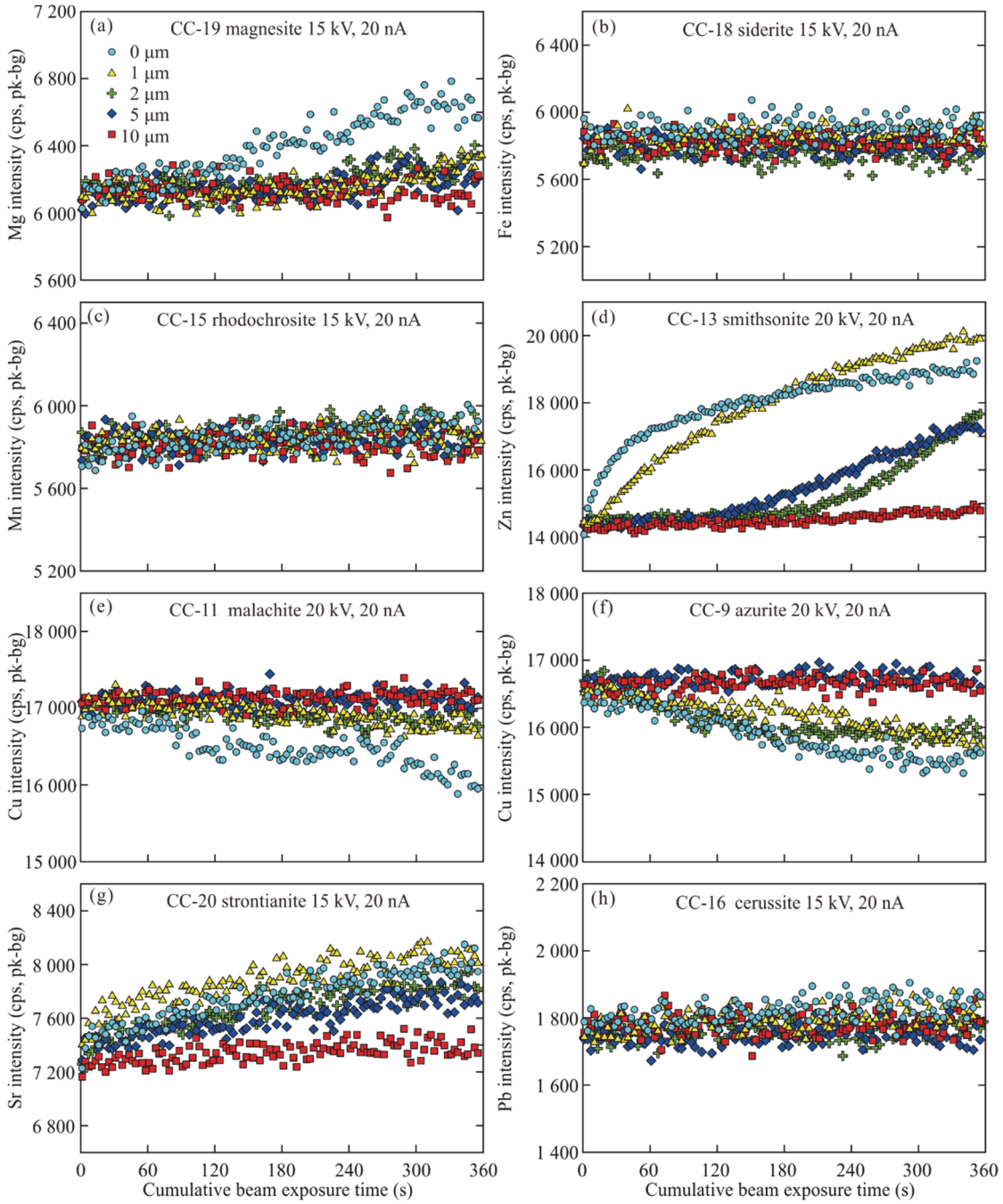

Figure 3. Effect of beam diameter on the X-ray TDI variations of Mg in magnesite (a), Fe in siderite (b), Mn in rhodochrosite (c), Zn in smithsonite (d), Cu in malachite (e), and azurite (f), Sr in strontianite (g), and Pb in cerussite (h).

For dolomite, we recorded the TDI variations of Ca, Mg, and C X-rays using beam currents of 5, 10, and 20 nA (Figs. 4c–4e). The Ca and Mg X-ray intensities increased steadily with the use of a 20 nA current, and remained constant with 10 and 5 nA currents (Figs. 4c, 4d). The C X-ray intensity in dolomite decreased steadily with 5, 10, and 20 nA beam currents, and most rapidly at 20 nA (Fig. 4e).

For other types of carbonate minerals, we investigated the time-dependent X-ray intensity variations of element M under 5, 10, 20, and 50 nA beam currents, and the results are shown in Fig. 5. Under beam currents of 5 and 10 nA, the X-ray intensities of Mg in magnesite (Fig. 5a), Fe in siderite (Fig. 5b), Mn in rhodochrosite (Fig. 5c), Zn in smithsonite (Fig. 5d), Cu in malachite (Fig. 5e), Cu in azurite (Fig. 5f), Sr in strontianite (Fig. 5g), and Pb in cerussite (Fig. 5h) remained constant. When using a beam current of 20 nA, the X-ray intensities of Zn in smithsonite and Sr in strontianite increased steadily whereas those of M elements in other carbonate minerals remained constant. Under a beam current of 50 nA, the X-ray intensities of Fe in siderite and Pb in cerussite remained constant whereas those of M elements in other carbonates showed some fluctuations.

Hence, the TDI variations of M elements in carbonate minerals varied more slowly at low beam currents, which is consistent with previous studies of glass and apatite (Goldoff et al., 2012; Morgan and London, 2005; Morgan and London, 1996; Stormer et al., 1993).

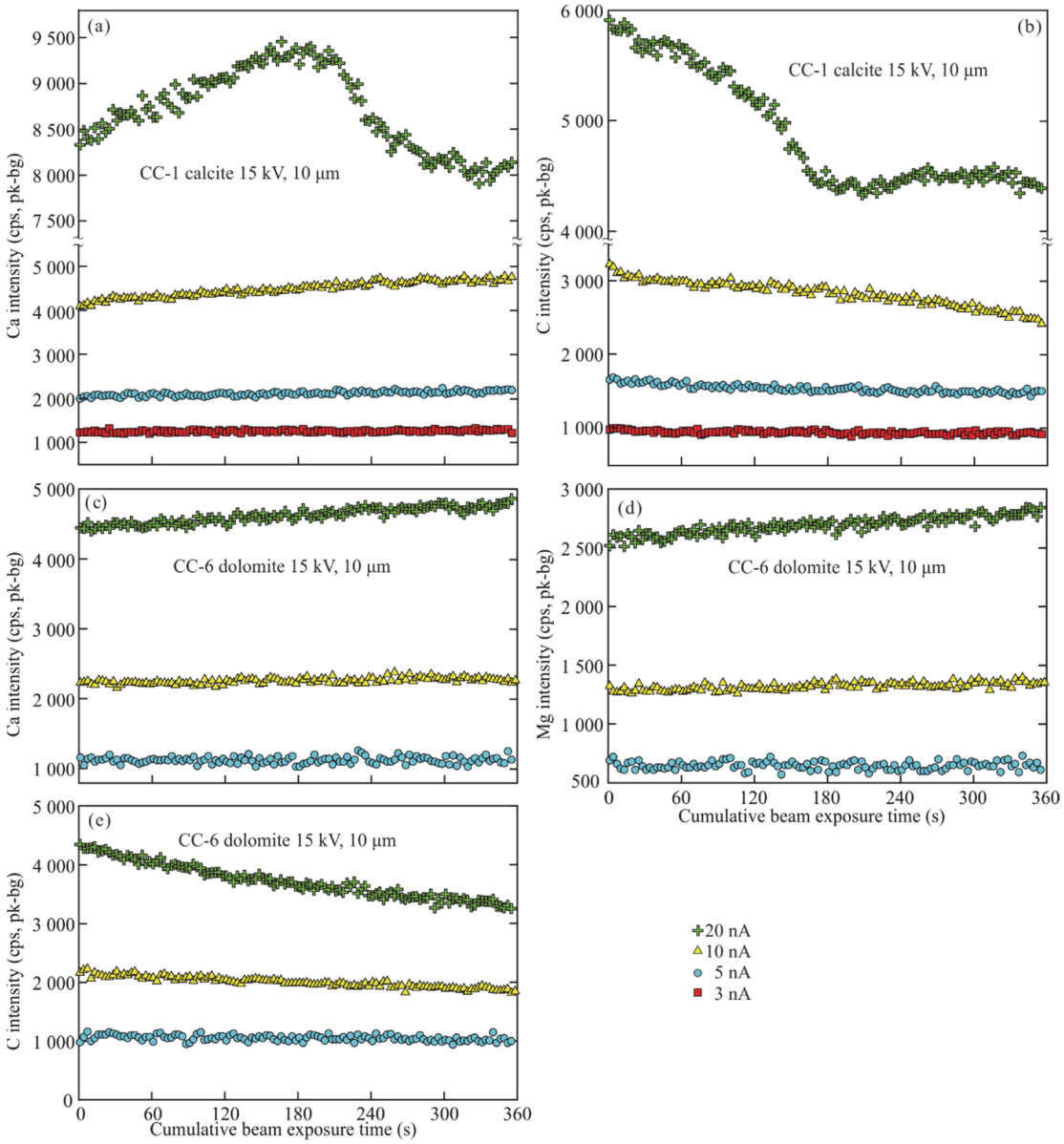

Figure 4. Effect of beam current on the X-ray TDI variations of Ca and C in calcite (a)–(b), and Ca, Mg, and C in dolomite (c)–(e).

2.4 Differences in the TDI Variation of Elemental X-Rays in Various Carbonate Minerals

In order to examine the differences in the TDI variation of a specific elemental X-ray in various carbonate minerals, we investigated the TDI variations of Ca in five calcite samples and three dolomite samples, Mg in three dolomite samples and one magnesite sample, and Zn in two smithsonite samples, under the same conditions. The results shown in Fig. 6 were obtained by setting the first intensity value as 1 and dividing the other data by the first value. Using a beam diameter of 20 μm and a beam current of 10 nA, the five calcite samples showed different time-dependent fluctuations of the Ca X-ray intensity (Fig. 6a). For example, in sample CC-2, the Ca X-ray intensity increased rapidly by 15% over 360 s, whereas it remained constant in sample CC-3. Under a beam diameter of 10 μm and a beam current of 20 nA, different Ca X-ray TDI variations were also observed in two calcite and three dolomite samples (Fig. 6b). A comparison between dolomite and magnesite samples showed that the Mg X-ray intensity in three dolomite samples increased with time, whereas it remained constant in the magnesite samples (Fig. 6c). Different Zn X-ray TDI variations were also observed in two different smithsonite samples under a beam diameter of 1 or 2 μm and a beam current of 20 nA (Fig. 6d). In summary, different X-ray TDI fluctuations were observed for a specific element in various carbonate minerals.

2.5 An Optimized Procedure for EPMA of Carbonate Minerals

EPMA with a small beam spot provides a high spatial resolution, and the use of a large beam current can improve the characteristic elemental X-ray intensity. However, small beam spot and/or large beam current can cause element migration or sample damage, leading to TDI variations of elemental X-rays in some materials. Various methods have been developed to minimize sample damage and reduce the X-ray intensity fluctuations, including increasing (or decreasing) accelerating voltage, reducing the beam current, increasing the beam spot size, the use of metal coatings to increase the thermal conductivity, sample motion during analysis, and TDI correction during analysis (Kearns and Ben, 2016; Kearns et al., 2014; Meier et al., 2011; Morgan and London, 2005; Smith, 1986).

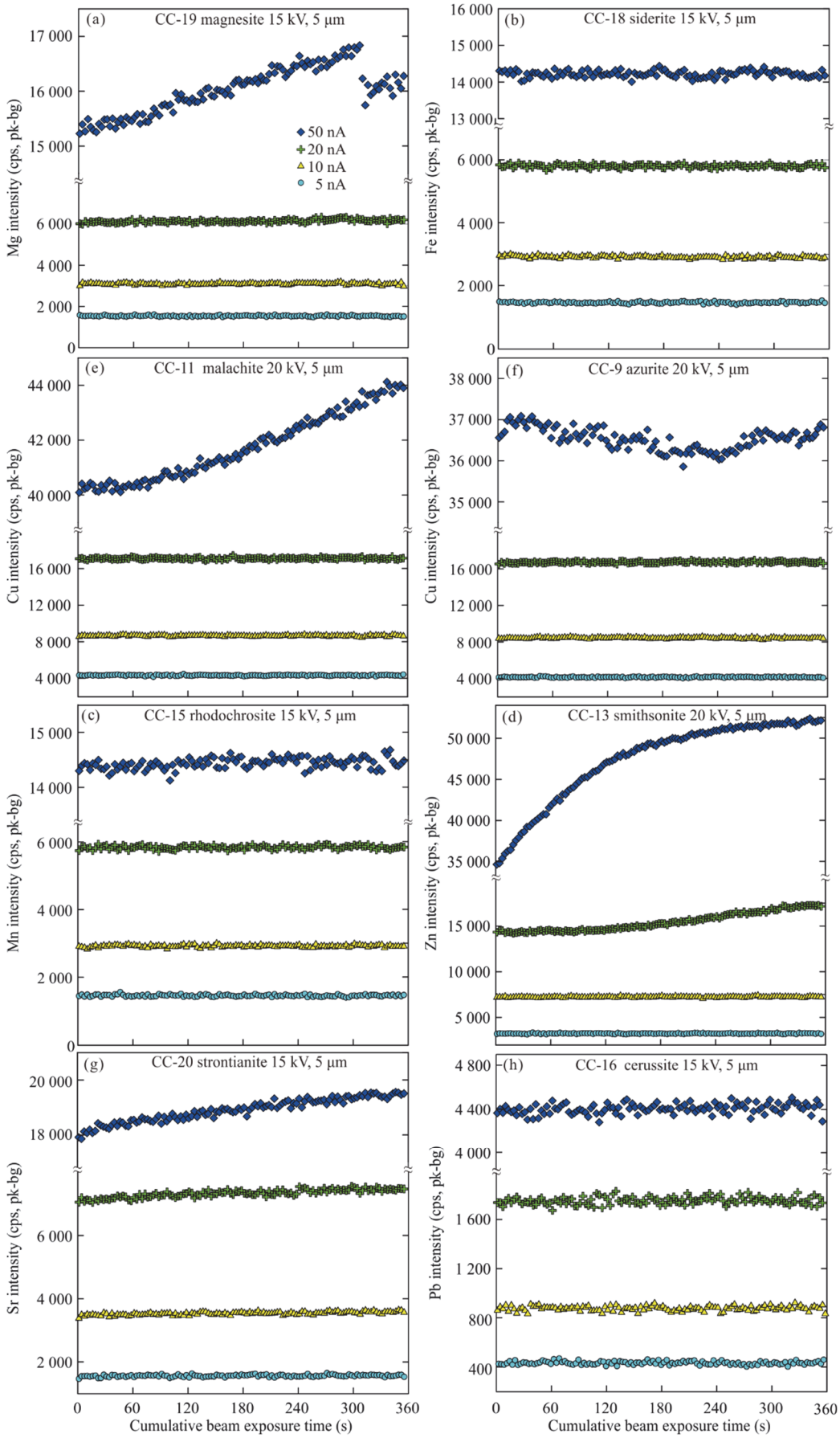

Figure 5. Effect of beam current on the X-ray TDI variations of Mg in magnesite (a), Fe in siderite (b), Mn in rhodochrosite (c), Zn in smithsonite (d), Cu in malachite (e) and azurite (f), Sr in strontianite (g), and Pb in cerussite (h).

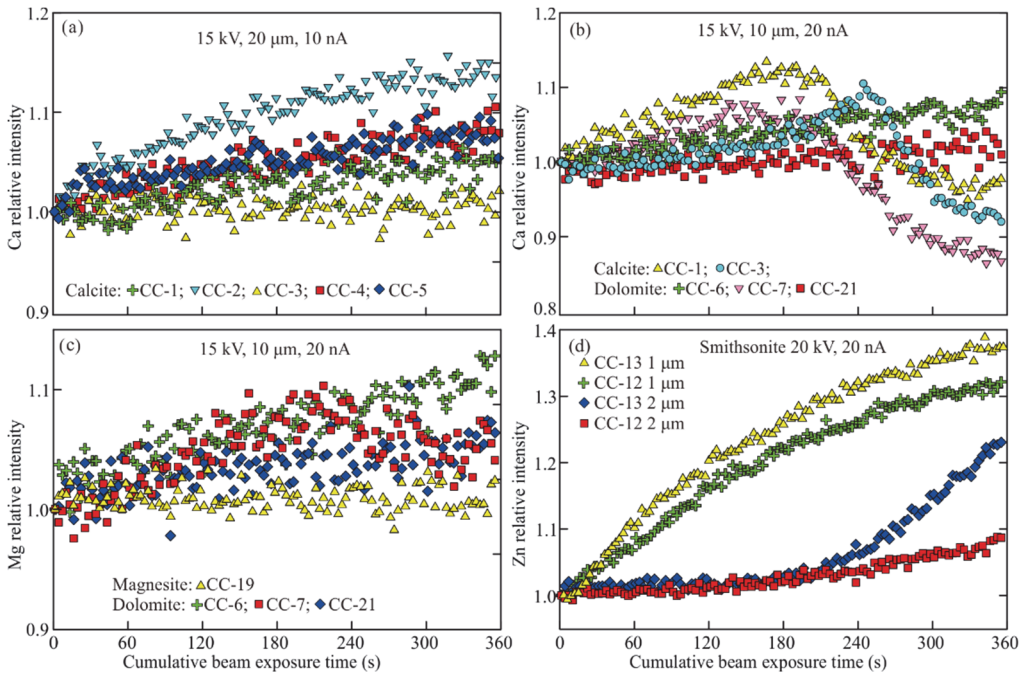

Figure 6. Differences in X-ray TDI fluctuations of Ca in five calcite samples (a), Ca in two calcite samples and three dolomite samples (b), Mg in three dolomite samples and one magnesite sample (c), and Zn in two smithsonite samples (d).

Based on this work, we developed an optimized EPMA procedure for carbonate minerals. For calcite, a beam current of 5 nA and a beam spot of 10 μm, which caused insignificant Ca X-ray TDI variations, were identified as optimal conditions (Fig. 4a). For the analysis of Ca and Mg in dolomite, the optimal conditions were 10 or 15 nA beam current and 10 μm beam spot (Fig. 4c). A 10 nA beam current and 5 μm beam spot or a 20 nA beam current and 10 μm beam spot were optimal for the EPMA of Sr in strontianite (Figs. 3g, 5g). For other carbonate minerals, a 20 nA beam current and a 5 μm beam spot gave the best results causing insignificant TDI variations of Mg in magnesite (Fig. 5a), Fe in siderite (Fig. 5b), Mn in rhodochrosite (Fig. 5c), Zn in smithsonite (Fig. 5d), Cu in malachite (Fig. 5e) and azurite (Fig. 5f), and Pb in cerussite (Fig. 5h).

Base on the studies above, the order of TDI fluctuation is Ca>Zn>Sr>Mg>Cu>Mn, Fe, Pb. The natural samples generally have completive components for the substitution between different cations. The higher the content of the elements with significant X-ray TDI variations, the smaller beam current and the larger beam spot size should be used. For analysis of carbonate minerals, elements with significant X-ray TDI variations should be examined first and reduce the counting time, followed by analysis of other minor and trace elements having small TDI fluctuations with increasing counting time. During image observation, a small current should be used to prevent element migration or sample damage due to electron beam irradiation. For small mineral grains or in the presence of mineral zoning, a small beam spot should be used; however, TDI variations under electron beam irradiation cannot be avoided, and TDI correction (Morgan and London, 1996; Stormer et al., 1993) is required.

To date, the use of silicate or carbonate minerals as a standard for carbonate microanalysis is controversial. An important requirement for standard materials is stability under electron beam irradiation (Carpenter, 2008; Sweatman and Long, 1969), and this study demonstrates that carbonate minerals do not meet this criterion. In addition, different TDI variations of an element were observed in carbonate minerals, and TDI variations in both standard and unknown samples under the same operating conditions cannot be compared. Hence, for EPMA of carbonate minerals, silicate minerals are preferred as standards rather than carbonate minerals.

3 CONCLUSION

An investigation of the effect of operating conditions on the time-dependent X-ray intensity variation for elements in carbonate minerals showed that the X-ray intensities of Ca in calcite and dolomite, Mg in dolomite, Zn in smithsonite, and Sr in strontianite were more sensitive to electron beam irradiation than other elements. A small current and a large beam diameter were found to minimize the time-dependent X-ray intensity variations, and the following optimal EPMA operating conditions were determined for various elements: 10 μm beam diameter and 5 nA current for calcite; 10 μm beam diameter and 10 or 15 nA current for dolomite; 5 μm beam diameter and 10 nA beam current or 10 μm beam diameter and 20 nA beam current for Sr in strontianite, and 20 nA beam current and 5 μm beam diameter for magnesite, siderite, rhodochrosite, smithsonite, malachite, azurite, and cerussite. The 15 kV accelerating voltage for Ca, Mg, Mn, Fe, Pb, and Sr, and 20 kV for Cu and Zn, are selected, due to that it produces robust X-ray counts for most elements analyzed. Elements sensitive to electron beam irradiation (Ca, Mg, Zn, and Sr) should be determined first, and counting time should be short, followed by longer counting times for trace and minor elements. a small beam current should be used during image observation. Moreover, for small mineral grains or in the presence of mineral zoning, a small beam spot should be used, and TDI correction is needed. In addition, silicate minerals are recommended as standards rather than carbonate minerals.

ACKNOWLEDGMENTS

This work was supported by the Natural Science Foundation of China (No. 41403022) and the Fundamental Research Funds for the Central Universities, China University of Geosciences (Wuhan) (No. CUGL150401). We are grateful to two anonymous reviewers for providing valuable comments and suggestions, which helped to improve this manuscript significantly. The final publication is available at Springer via https://doi.org/10.1007/s12583-017-0939-x.

REFERENCES CITED

Carpenter, P., 2008. EPMA Standards: The Good, the Bad, and the Ugly. *Microscopy and Microanalysis*, 14(S2): 530–531. https://doi.org/10.1017/s1431927608088740

Essene, E. J., 1983. Solid Solutions and Solvi among Metamorphic Carbonates with Applications to Geologic Thermobarometry. *Reviews in Mineralogy*, 11(1): 77–96

Goldoff, B., Webster, J. D., Harlov, D. E., 2012. Characterization of Fluor-Chlorapatites by Electron Probe Microanalysis with a Focus on Time-Dependent Intensity Variation of Halogens. *American Mineralogist*, 97(7): 1103–1115. https://doi.org/10.2138/am.2012.3812

Henderson, C., 2011. Beam Sensitivity in EPMA: The Analysis of Apatite, $Ca_5(PO_4)_3$ (F, Cl, OH). *Microscopy and Microanalysis*, 17(S2): 588–589. https://doi.org/10.1017/s1431927611003813

Humphreys, M. C. S., Kearns, S. L., Blundy, J. D., 2006. SIMS Investigation of Electron-Beam Damage to Hydrous, Rhyolitic Glasses: Implications for Melt Inclusion Analysis. *American Mineralogist*, 91(4): 667–679. https://doi.org/10.2138/am.2006.1936

Jurek, K., Gedeon, O., 2003. Analysis of Alkali-Silicate Glasses by Electron Probe Analysis. *Spectrochimica Acta Part B*: *Atomic Spectroscopy*, 58(4): 741–744. https://doi.org/10.1016/s0584-8547(02)00288-4

Kearns, S. L., Ben, B. S., 2016. Low Voltage FEG-EPMA in Earth Sciences—Problems and Solutions for Analysis of Unstable Materials. *Microscopy and Microanalysis*, 22(S3): 416–417. https://doi.org/10.1017/s1431927616002932

Kearns, S., Ben, B. S., Wade, J., 2014. Mitigating Thermal Beam Damage with Metallic Coats in Low Voltage FEG-EPMA of Geological Materials. *Microscopy and Microanalysis*, 20(S3): 740–741. https://doi.org/10.1017/s143192761400542x

Kerrick, D. M., Eminhizer, L. B., Villaume, J. F., 1973. The Role of Carbon Film Thickness in Electron Microprobe Analysis. *American Mineralogist*, 58(9/10): 920–925

Lane, S. J., Dalton, J. A., 1994. Electron Microprobe Analysis of Geological Carbonates. *American Mineralogist*, 79(7/8): 745–749

Marks, M. A. W., Wenzel, T., Whitehouse, M. J., et al., 2012. The Volatile Inventory (F, Cl, Br, S, C) of Magmatic Apatite: An Integrated Analytical Approach. *Chemical Geology*, 291: 241–255. https://doi.org/10.1016/j.chemgeo.2011.10.026

McGee, J. J., Keil, K., 2001. Application of Electron Probe Microanalysis to the Study of Geological and Planetary Materials. *Microscopy and Microanalysis*, 7(2): 200–210

Meier, D. C., Davis, J. M., Vicenzi, E. P., 2011. An Examination of Kernite ($Na_2B_4O_6(OH)_2{\cdot}3H_2O$) Using X-Ray and Electron Spectroscopies: Quantitative Microanalysis of a Hydrated Low-Z Mineral. *Microscopy and Microanalysis*, 17(5): 718–727. https://doi.org/10.1017/s1431927611000602

Morgan, G. B., London, D., 1996. Optimizing the Electron Microprobe Analysis of Hydrous Alkali Aluminosilicate Glasses. *American Mineralogist*, 81(9/10): 1176–1185. https://doi.org/10.2138/am-1996-9-1016

Morgan, G. B. IV, London, D., 2005. The Effect of Current Density on the Electron Microprobe Analysis of Alkali Aluminosilicate Glasses. *American Mineralogist*, 90(7): 1131–1138. https://doi.org/10.2138/am.2005.1769

Smith, M. P., 1986. Silver Coating Inhibits Electron Microprobe Beam Damage of Carbonates. *Journal of Sedimentary Research*, 56(4): 560–561. https://doi.org/10.1306/212f89c7-2b24-11d7-8648000102c1865d

Spray, J. G., Rae, D. A., 1995. Quantitative Electron-Microprobe Analysis of Alkali Silicate Glasses: A Review and User Guide. *The Canadian Mineralogist*, 33(2): 323–332

Stock, M. J., Humphreys, M. C. S., Smith, V. C., et al., 2015. New Constraints on Electron-Beam Induced Halogen Migration in Apatite. *American Mineralogist*, 100(1): 281–293. https://doi.org/10.2138/am-2015-4949

Stormer, J. C., Pierson, M. L., Tacker, R. C., 1993. Variation of F and Cl X-Ray Intensity due to Anisotropic Diffusion in Apatite during Electron Microprobe Analysis. *American Mineralogist*, 78(5–6): 641–648

Sweatman, T. R., Long, J. V. P., 1969. Quantitative Electron-Probe Microanalysis of Rock-Forming Minerals. *Journal of Petrology*, 10(2): 332–379. https://doi.org/10.1093/petrology/10.2.332

Yang, S. Y., Jiang, S. Y., 2012. Chemical and Boron Isotopic Composition of Tourmaline in the Xiangshan Volcanic-Intrusive Complex, Southeast China: Evidence for Boron Mobilization and Infiltration during Magmatic-Hydrothermal Processes. *Chemical Geology*, 312/313: 177–189. https://doi.org/10.1016/j.chemgeo.2012.04.026

Yang, S. Y., Jiang, S. Y., 2013. Occurrence and Significance of a Quartz-Amphibole Schist Xenolith within a Mafic Microgranular Enclave in the Xiangshan Volcanic-Intrusive Complex, SE China. *International Geology Review*, 55(7): 894–903. https://doi.org/10.1080/00206814.2012.752662

Yang, S. Y., Jiang, S. Y., Palmer, M. R., 2015a. Chemical and Boron Isotopic Compositions of Tourmaline from the Nyalam Leucogranites, South Tibetan Himalaya: Implication for Their Formation from B-Rich Melt to Hydrothermal Fluids. *Chemical Geology*, 419: 102–113. https://doi.org/10.1016/j.chemgeo.2015.10.026

Yang, S. Y., Jiang, S. Y., Zhao, K. D., et al., 2015b. Tourmaline as a Recorder of Magmatic-Hydrothermal Evolution: An *in-situ* Major and Trace Element Analysis of Tourmaline from the Qitianling Batholith, South China. *Contributions to Mineralogy and Petrology*, 170(5/6): 1–21. https://doi.org/10.1007/s00410-015-1195-7

Ye, M., Zhao, H., Zhao, M., et al., 2017. Mineral Chemistry of Biotite and Its Petrogenesis Implication in Lingshan Granite Pluton, Gan-Hang Belt, SE China. *Acta Petrologica Sinica*, 33(3): 896–906 (in Chinese with English Abstract)

Zhang, R. X., Yang, S. Y., 2016. A Mathematical Model for Determining Carbon Coating Thickness and Its Application in Electron Probe Microanalysis. *Microscopy and Microanalysis*, 22(6): 1374–1380. https://doi.org/10.1017/s143192761601182x

Zhang, H. C., Zhu, Y. F., Feng, W. Y., et al., 2017. Paleozoic Intrusive Rocks in the Nalati Mountain Range (NMR), Southwest Tianshan: Geodynamic Evolution Based on Petrology and Geochemical Studies. *Journal of Earth Science*, 28(2): 196–217. https://doi.org/10.1007/s12583-016-0922-1

Zhao, D. G., Zhang, Y. X., Essene, E. J., 2015. Electron Probe Microanalysis and Microscopy: Principles and Applications in Characterization of Mineral Inclusions in Chromite from Diamond Deposit. *Ore Geology Reviews*, 65: 733–748. https://doi.org/ 10.1016/j.oregeorev.2014.09.020

Zhao, L. M., Takasu, A., Liu, Y. J., et al., 2017. Blueschist from the Toudaoqiao Area, Inner Mongolia, NE China: Evidence for the Suture between the Ergun and the Xing'an Blocks. *Journal of Earth Science*, 28(2): 241–248. https://doi.org/10.1007/s12583-017-0721-0